Design and implementation of a maximal-ratio angle-diversity receiver for optical wireless communication systems

António M. R. Tavares, Rui J. M. T. Valadas, A. M. de Oliveira Duarte

University of Aveiro
Dept. of Electronics and Telecommunications / Institute of Telecommunications
3810 Aveiro, PORTUGAL
Fax: +351.34.381941   e-mail: tavares@zeus.ci.ua.pt

ABSTRACT

A maximal-ratio angle-diversity receiver is composed of multiple sectors with relatively small field-of-views. Each sector estimates the signal-to-noise ratio (SNR) of the collected signal and its gain made proportional to the relation i/σ^2, where i and σ represent the average signal and the shot noise root mean square (*rms*) values, respectively. The output signals of all sectors are then combined through an adder circuit. This paper presents the design and implementation of a maximal-ratio receiver using discrete components. A major challenge is the design of the variable gain amplifier (VGA) which requires a large dynamic range because of the large fluctuations of both signal and noise in a typical office room environment. This problem was overcome through the utilisation of a cascade of two VGAs where the assignment of gains to each VGA minimises dynamic range requirements through an innovative topology. The first one provides a gain inversely proportional to the rms shot noise and the second one a gain proportional to the SNR referred to the input of the front-end. Measurements on an implemented prototype show results close to the ideal gain of a maximal-ratio receiver making the proposed techniques suitable for maximal-ratio angle-diversity receivers.

Keywords: infrared wireless communications, angle-diversity receiver, diversity, infrared, indoor wireless communications.

1. INTRODUCTION

The performance of wireless indoor infrared (IR) communication systems is impaired by several aspects. One of the most important is the existence of optical noise sources in the transmission channel. In typical rooms there are, usually, large quantities of IR illumination originated from sun light, incandescent lamps and fluorescent lamps which induces optical noise into optical receivers[1-4]. Also, indoor IR transmission systems are degraded by multipath dispersion.

Usually, receivers for IR communication systems are based on a single optical detector. This may be a good configuration in environments where both, signal and noise are isotropic. However, in most environments the transmitted signal illuminates the receiver from privileged directions. Also, the ambient light noise emanates from particular directions coinciding with the position of lamps or windows. Moreover, these light sources are, usually, in the receiver field-of-view (FOV). These characteristics provoke large variations on the signal-to-noise ratio (SNR), depending on the position, orientation and radiation pattern of both signal and noise sources and on the position, orientation and FOV of the receiver.

To minimise the effects of SNR fluctuations, several receiver techniques were proposed[4-6]. Gfeller[4] proposed an adaptive data rate receiver, where the data rate is continuously adjusted with the purpose of maintaining full network connectivity, trading-off speed and range. Valadas[5] proposed the use of an angle-diversity receiver which was shown to reduce significantly the optical penalty induced by ambient noise[5,7]. More recently, Tang[6] studied the combined use of multi-beam transmitters and angle-diversity receivers, based on a single imaging concentrator coupled with a segmented photodetector, showing also significant optical gains. Angle-diversity showed, also, to be very effective in combating multipath dispersion[8].

An angle-diversity receiver is composed by multiple sectors (optical receivers) with a relatively small FOV. Each sector estimates the SNR of the collected signal. The gain of a sector is proportional to i/σ^2, where i and σ represent the average signal and root mean square (*rms*) noise values, respectively. In the case of a maximal-ratio receiver, the output signals of all sectors are combined through an adder circuit. This contrasts with best sector receivers where only the sector with the best SNR is selected.

The structure of the maximal-ratio angle-diversity receiver is illustrated in figure 1. This receiver comprises one front-end, one circuit to estimate the SNR and a variable gain amplifier (VGA) per sector. The output signals of all sectors are combined through an adder circuit.

This paper presents the design and implementation of a maximal-ratio angle-diversity receiver prototype. In this paper we concentrate on an implementation of a single sector using discrete components. Section 2 presents the design and implementation aspects of the sector. In section 3, we present and discuss the results achieved with the implemented VGA. The main conclusions of this work are presented in section 4.

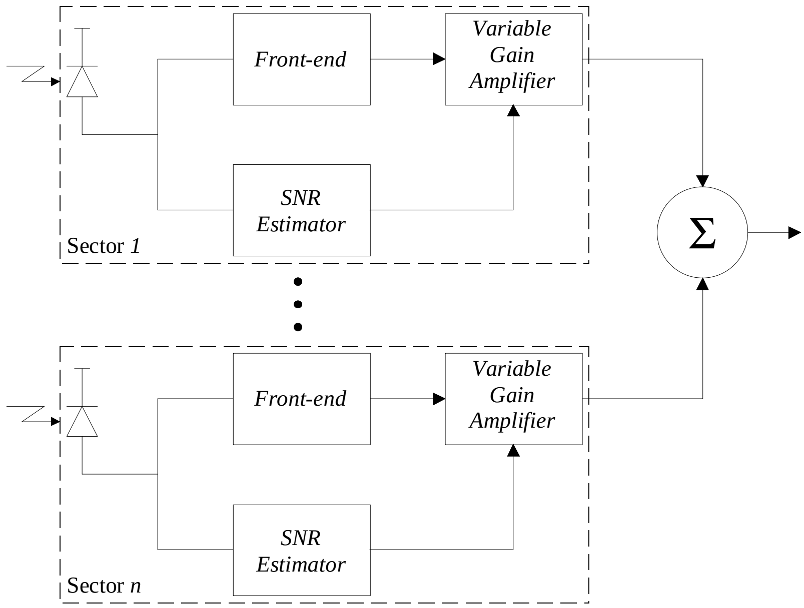

Figure 1. Structure of a maximal-ratio angle-diversity receiver.

2. DESIGN OF THE OPTICAL SECTOR

The design of the optical sector comprises the project of the optical front-end, SNR estimation circuits and variable gain amplifiers. During the design of the optical sector we will ignore the optical interference induced by the artificial light, the photodetector bulk and surface dark currents and the thermal noise associated with the bias resistor. So, the photodiode output current can be described by

$$i(t) = i_S(t) + I_{p_{dc}} + i_N(t) \tag{1}$$

where $i_S(t)$ is the desired signal, $I_{p_{dc}}$ is the stationary photocurrent and $i_N(t)$ is the shot noise current with the mean square value, σ^2, proportional to the current $I_{p_{dc}}$. Considering that the shot noise from ambient light is the dominant noise source and neglecting all other noise sources, the signal at the front-end output can be described by

$$v(t) = v_S(t) + v_N(t) \tag{2}$$

where $v_S(t)$ is the desired signal and $v_N(t)$ is the shot noise voltage at the output of the front-end. We will always refer the amplitude of the desired signal by V_S. For simplicity, instead of $i_S(t)$, $i_N(t)$, $v_S(t)$ and $v_N(t)$ we will use i_S, i_N, v_S and v_N, respectively.

The goal of the maximal-ratio angle-diversity receiver is to reduce the penalty induced by stationary photocurrent arising from the ambient light sources ignoring the optical interference produced by artificial light. Moreira[9] verified that fluorescent lamps driven by conventional ballasts produce very strong optical and electrical interference with spectra up to several kHz and that the interference produced by fluorescent lamps geared by electronic ballasts extends to more that 1 MHz. Consequently, the assumption of a stationary quantum noise is the major limitation of this work. In truth, during the bit slot time the quantum noise could be considered stationary, but it could vary significantly during the interference period. During the design of the optical sector, it was assumed that the penalty associated to the optical interference could be reduced through the utilisation of an appropriate encoding method, and through the utilisation of adequate electrical and optical filtering[10,11].

2.1 Design of the optical front-end

In addition to thermal noise, shot noise and optical interference, there is another signal degrading factor caused by the electromagnetic interference (EMI). To reduce the effects of the EMI, the infrared receiver was separated in two complementary low noise transimpedance amplifiers. The design of the optical front-end followed the one presented by Tavares[3]. It was projected to operate at 1 Mbps using Manchester line coding. A block diagram of the IR receiver is shown in figure 2. The IR receiver includes two arrays of PIN photodiodes, two differential low noise transimpedance amplifiers and a differential amplifier followed by a VGA. Each photodetector array is composed by five PIN photodiodes (A_r = 7 mm^2, FOV = 60°) corresponding to a total active area of 0.35 cm^2 per photodetector array. The IR receiver is separated in two differential low noise transimpedance amplifiers with a transimpedance gain of about 550 $k\Omega$. Following each transimpedance amplifier, there is a second order low-pass filter. This active filter is an approximation to a raised cosine shaping filter to minimise the intersymbol interference. The difference between the complementary outputs is accomplished by a differential amplifier. The purpose of the VGA which follows the differential amplifier is to exhibit an output signal proportional to $(SNR)^2$.

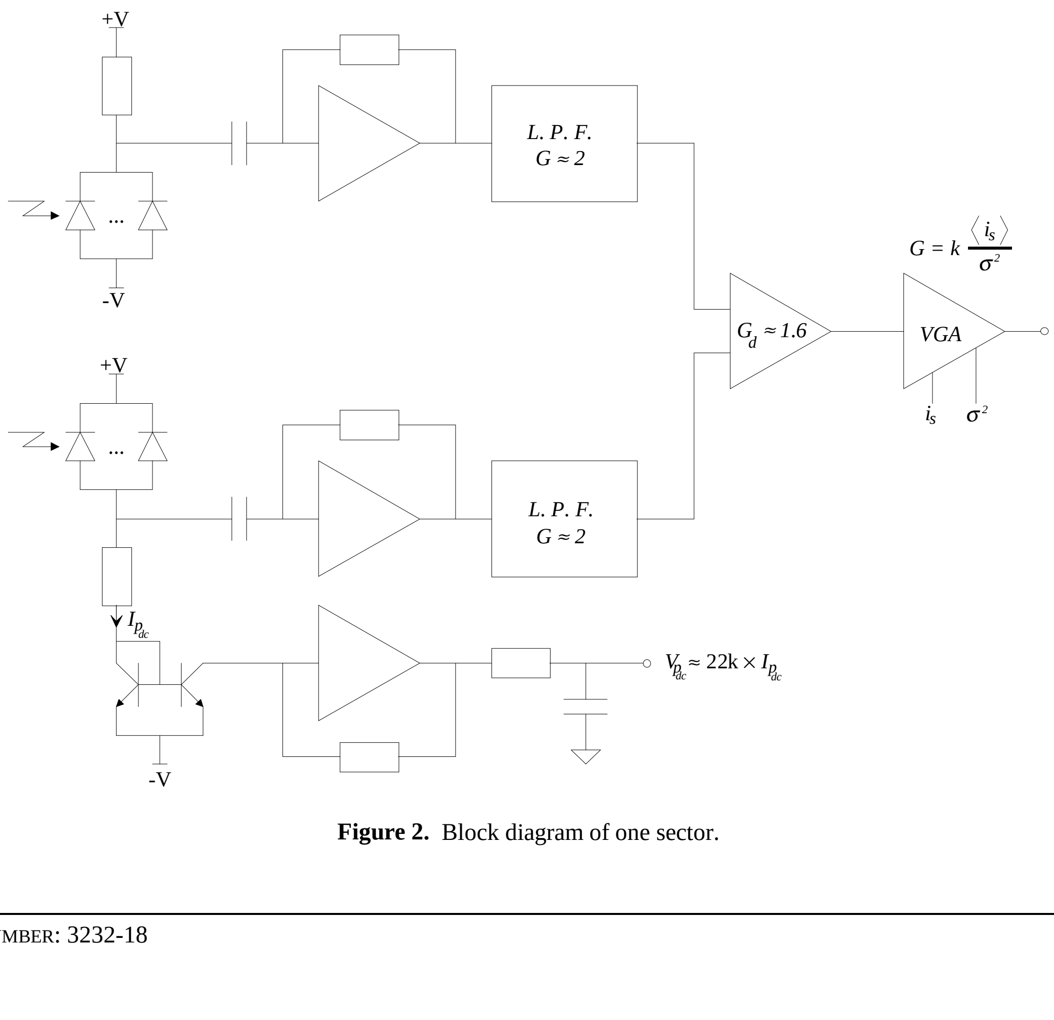

Figure 2. Block diagram of one sector.

2.2 Design considerations of the VGA

The gain of each sector in a maximal-ratio receiver must be proportional to the relation i / σ^2, and can be described by

$$G = k \frac{\langle i_S \rangle}{\sigma^2} \tag{3}$$

where $\langle i_S \rangle$ and σ^2 are the average desired signal and the shot noise mean square values referred to the input of the front-end, respectively, and k is a scale factor characteristic of the receiver. Thus, the signal amplitude obtained at the output of each sector is proportional to the square of the SNR and can be given by

$$V_{S_o} = k\left(\frac{\langle i_S \rangle}{\sigma}\right)^2 = k \times (\mathrm{SNR})^2 \tag{4}$$

The variance of the input-referred noise (shot noise), accounting the pulse shaping after the preamplifier, is proportional to the average value of the *dc* (direct current) photocurrent $I_{p_{dc}}$ and is given by[1]

$$\sigma^2 = 2qI_2 I_{p_{dc}} B \tag{5}$$

where q is the electronic charge of an electron, B is the bit rate and I_2 is a noise bandwidth factor depending of the transmitter pulse shape and equalised pulse shape only. For our receiver implementation $I_2 = 0.562$. Once the shot noise mean square value is proportional to the *dc* photocurrent, the gain of the VGA, represented by equation 3, can be given by

$$G = k \frac{\langle i_s \rangle}{I_{p_{dc}}} \tag{6}$$

To implement the desired gain it is necessary to evaluate $I_{p_{dc}}$. Since the complementary photodiode arrays are placed near enough, the *dc* photocurrent induced on both photodiode arrays is almost identical. So, the measurement of $I_{p_{dc}}$ can be only performed on one branch of the differential front-end. Figure 2 illustrates the evaluation of $I_{p_{dc}}$ which was executed through the inclusion of a current mirror into the photodiode bias circuit.

During the project of the desired VGA it must be taken into account that the optical transmission channel has a large optical range both in terms of signal and noise. These characteristics demand a large dynamic range in the VGA. A series of measurements of the photocurrent density were presented by Gfeller[1] showing that a predominantly daylight environment generates an induced *dc* photocurrent density of about 150 $\mu A/cm^2$ into a silicon photodiode with an active area of 1 cm^2 and FOV = 50°. This value was measured near windows but with the photodiode not exposed to direct sunlight. The same *dc* photocurrent was also obtained with the photodiode placed under a 75 *W* tungsten desk lamp at a distance of 65 *cm*. Also, these measurements showed that, under a well illuminated room, the ambient light noise varies over several orders of magnitude. This illumination could produce an induced photocurrent density varying from 3 $\mu A/cm^2$ up to 1 mA/cm^2. Another set of measurements of the photocurrent density were presented considering typical well illuminated environments[3] and was verified that the *dc* photocurrent induced into a PIN photodiode was larger than 12 $\mu A/cm^2$. When the photodiode was placed near windows this value increased to about 1.2 mA/cm^2. These measurements were executed with a PIN photodiode with an active area of 0.85 cm^2 and FOV = 85°. So, taking into account these measurements[1,3], the VGA must be projected to operate rightly for an induced *dc* photocurrent from about 12 $\mu A/cm^2$ up to about 1.2 mA/cm^2. Then, considering a signal irradiance corresponding to an electrical dynamic range of about 40 *dB* and that the *dc* photocurrent varies between the range previously presented, it is required a VGA with a functional dynamic range of

$$DR_{VGA} = \frac{\langle i_{S_{\max}} \rangle}{\langle i_{S_{\min}} \rangle} \times \frac{\sigma_{\max}^2}{\sigma_{\min}^2} = 80\ dB \tag{7}$$

which is difficult to implement. This problem can be relaxed through the utilisation of a cascade of two VGAs. Figure 3 illustrates this option and identifies some signals used during the design of the VGAs.

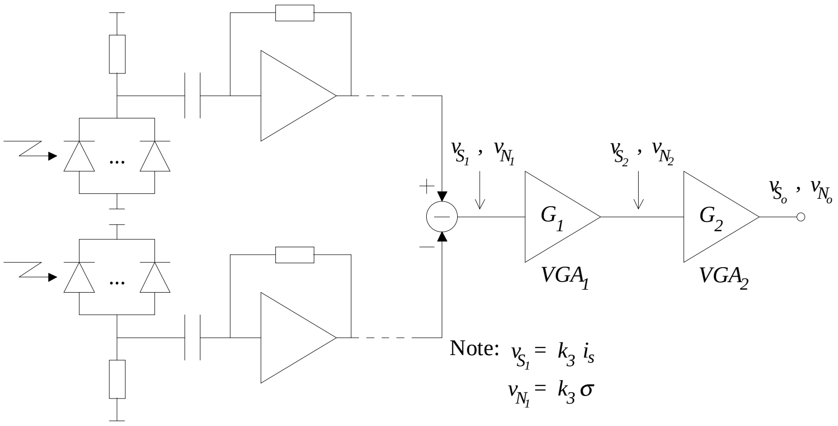

Figure 3. Block diagram of one sector with two VGAs.

Now we have to decide on which gain should be assigned to each VGA. As the VGA is controlled by two distinct signals, $\langle i_S \rangle$ and $I_{p_{dc}}$, the easiest option would be to have $G_1 = k\langle i_S \rangle$ and $G_2 = k/\sigma^2$, where G_1 and G_2 are the gains of the first and of the second VGA, respectively. However, this option still requires a large VGA dynamic range. Indeed, the required VGA dynamic range would be of 40 *dB* in each VGA. An ingenious alternative is to define

$$G_1 = \frac{k_1}{\sigma} \tag{8}$$

and

$$G_2 = k_2 \times V_{S_2} \tag{9}$$

where V_{S_2} is the amplitude of the signal at the input of the second VGA. This option is more complicated because it requires a square root circuit but, as we demonstrate, the obtained profits compensate the complexity. With this implementation, the dynamic range of the first VGA (VGA_1) will be

$$DR_{VGA_1} = \frac{\sigma_{\max}}{\sigma_{\min}} = \frac{\sqrt{I_{p_{dc\_\max}}}}{\sqrt{I_{p_{dc\_\min}}}} = 20\ dB \tag{10}$$

which can be easily implemented. Then, the average output signal of VGA_1, $\langle v_{S_2} \rangle$, will be proportional to the SNR

$$\langle v_{S_2} \rangle = \langle i_S \rangle A_{FE}\, G_1 = k \cdot SNR \tag{11}$$

where A_{FE} is the front-end gain. Obviously, the shot noise *rms* value at the output of VGA_1, $\langle v_{N_2} \rangle$, will be the same for all sectors

$$\langle v_{N_2} \rangle = \sigma A_{FE} G_1 = k \tag{12}$$

In the particular situation where all the branches of a maximal-ratio sectored receiver have the same input noise the ideal gain in each sector must be $G = k \cdot \langle i_S \rangle$. Since these conditions happen at the input of the second VGA (VGA_2) it is obvious that the gain of VGA_2 must be proportional to the amplitude of its input signal, as given in equation 9. In other words, the gain of VGA_2 is proportional to the SNR. So, the required dynamic range of VGA_2 is only limited by the maximum and minimum SNR which will be reasonable to consider. In optical transmission systems it is usual to define the receiver sensitivity as the minimum irradiance required to achieve a bit error rate (BER) of 10^{-9}. In our receiver this BER corresponds to $\mathrm{SNR} = 6/\sqrt{2}$ (referred to one input of the differential front-end). We will use this value as a reference value during the design of the second VGA. For a SNR double and half of the reference value, the corresponding bit error rate is about 1.8×10^{-33} and 1.3×10^{-3}, respectively. These values can be considered large and small enough to define the maximum and minimum SNR where the gain of VGA_2 must increase linearly with the SNR. So, the required linear dynamic range of VGA_2 would be of about 12 *dB* $\left(20 \cdot \log\left(SNR_{MAX}/SNR_{MIN}\right)\right)$. However, the results presented in a previous paper[3] showed that there was a difference of about 8.2 *dB* between the theoretical and the measured sensitivity. This difference was caused by the optical interference produced by artificial light sources (fluorescent lamps). So, taking into account these results[3], we decide to increase the maximum SNR, previously defined, by a factor of 6.6 (8.2 *dB*). Thus, the gain of VGA_2 must increase linearly from $\mathrm{SNR} = 3/\sqrt{2}$ until, at least, a SNR of about 56 and, the dynamic range of VGA_2 will be of about 28 *dB*. This dynamic range may be excessive. This subject is for further study.

Finally, through the utilisation of the cascade of the two VGAs, the global gain is

$$G = \frac{V_{S_O}}{\langle i_S \rangle} = \frac{G_2 V_{S_2}}{\langle i_S \rangle} = \frac{k_2 \left(G_1 V_{S_1}\right)^2}{\langle i_S \rangle} = \frac{k_2 \left(\frac{k_1}{\sigma} k_3 \langle i_S \rangle\right)^2}{\langle i_S \rangle} = k \frac{\langle i_S \rangle}{\sigma^2} \tag{13}$$

as it was required and described in equation 3. In equation 13, V_{S_1} is the amplitude value of the v_{S_1} signal.

2.3 Project and implementation aspects of the first VGA

As it was previously referred, the gain of VGA_1 (equation 8) is inversely proportional to the *rms* value of the shot noise current which means that G_1 is inversely proportional to the square root of $I_{p_{dc}}$. So, the aim of the VGA_1 is to implement, as close as possible, the following equation

$$G_1 = \frac{k}{\sqrt{I_{p_{dc}}}} \tag{14}$$

Figure 4 shows the block diagram of the first VGA containing three main blocks: a divide circuit, a square root circuit and an offset voltage adder circuit. The square root circuit is implemented by the introduction of a multiplier circuit, with its inputs connected together, in the feedback path of an operational amplifier. This block implements the following square root function

$$V_B = \sqrt{10\ V_A} \tag{15}$$

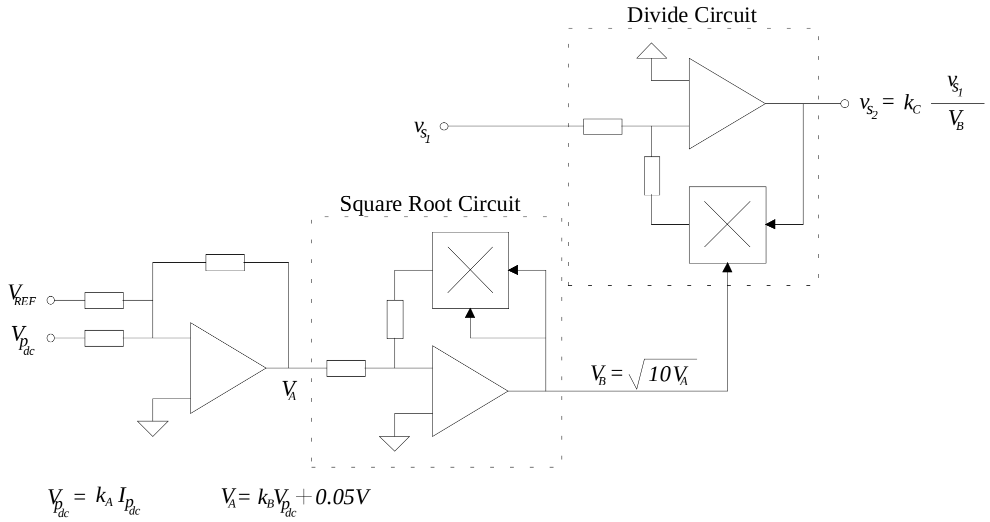

Figure 4. Block diagram of the VGA$_1$.

In the divide circuit a multiplier is placed on the feedback path of an operational amplifier. One of the multiplier input is the denominator, V_B, and the other one is connected to the output of the amplifier. This block implements the divide function presenting the following output

$$v_{S_2} = k_C \frac{v_{S_1}}{V_B} \tag{16}$$

To guarantee that the denominator of the divide circuit is different from zero even when no illumination is present ($I_{p_{dc}} \approx 0$), a *dc* reference voltage (V_{REF}) was added, to the *dc* voltage $V_{p_{dc}}$, through an offset adder circuit. To increase the accuracy of the square root circuit, the offset voltage must be as small as possible. However, insignificant values of the optical illumination and small values of the offset voltage can provoke the saturation of the divide circuit. The project of this reference voltage was done trading-off the optimum design and the practical implementation and assuring that the offset voltage causes a small deviation between the ideal square root function and the implemented one. Choosing an offset voltage of 0.05 *V*, for a *dc* photocurrent of about 12 $\mu A/cm^2$ the result of the implemented square root operation will be deviated by about 12% from the ideal square root value. For larger values of $I_{p_{dc}}$ the difference between projected and theoretical square root values is reduced increasing the accuracy of the implemented gain G_{1_p} (first branch of equation 17). In section 2.2, we referred that the VGA would operate correctly between 12 $\mu A/cm^2$ and 1.2 mA/cm^2 which is preserved with this implementation. In our design, for $\text{SNR} \geq 198$ the output of the VGA$_1$ saturates and the resulting gain G_{1_p} can be expressed by the second branch of the following equation

$$G_{1_p} = \begin{cases} -\dfrac{k_C}{\sqrt{10\left(k_A k_B I_{p_{dc}} + 0.05\right)}} & \text{if} \quad \text{SNR} < 198 \\ -\dfrac{2.64 \times 10^{-6}}{\left\langle i_S \right\rangle} & \text{if} \quad \text{SNR} \geq 198 \end{cases} \tag{17}$$

where the constants k_A, k_B and k_C resulting from the project are about 22×10^3, 2.17 and 10, respectively.

2.4 Project and implementation aspects of the second VGA

Figure 5 illustrates the block diagram of the second VGA which consists of two main blocks: a peak detector and a multiplier circuit.

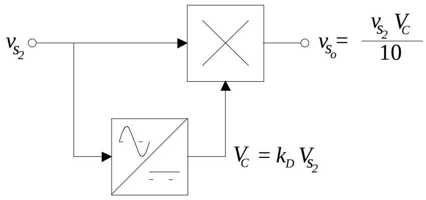

Figure 5. Block diagram of the VGA_2.

The peak detector estimates the amplitude value of the signal, v_{S_2}, present at the output of the VGA_1. So, the gain of the VGA_2 is proportional to the SNR, as required. In our implementation $k_D \cong 3.6$ and the resulting G_{2_P} is defined by the first branch of equation 18. To satisfy the design considerations presented in section 2.2, the gain of VGA_2 was made proportional to V_{S_2} for a SNR < 60 (corresponding to $V_{S_2} = 2.75\text{V}$). For a SNR larger than 60, the gain of the second VGA remains constant and is described by the second branch of the following equation

$$G_{2_P} = \begin{cases} 0.36 \times V_{S_2} & \text{if} \quad V_{S_2} < 2.75V \quad (\text{or} \quad \text{SNR} < 60) \\ 0.985 & \text{if} \quad V_{S_2} \geq 2.75V \quad (\text{or} \quad \text{SNR} \geq 60) \end{cases} \tag{18}$$

2.5 Global VGA

The global gain achieved with the implementation of VGA_1 and VGA_2 can be defined by equation 19. It is expected that for SNR < 60 and for *dc* photocurrents larger than 12 $\mu A/cm^2$, this implementation approximates to the ideal gain described by equation 6.

$$G_p = \begin{cases} -\dfrac{12.74 \times 10^6 \times \langle i_S \rangle}{47.7 \times 10^3 I_{p_{dc}} + 0.05} & \text{if} \quad \text{SNR} < 60 \\ -\dfrac{9.85}{\sqrt{10\left(47.7 \times 10^3 I_{p_{dc}} + 0.05\right)}} & \text{if} \quad 60 \leq \text{SNR} < 198 \\ -\dfrac{2.6 \times 10^{-6}}{\langle i_S \rangle} & \text{if} \quad \text{SNR} \geq 198 \end{cases} \tag{19}$$

3. EXPERIMENTAL RESULTS

3.1 Experimental results of the first VGA

Figure 6 presents the gain of the first VGA versus *dc* photocurrent considering that this current varies from about 0 to 300 $\mu A/cm^2$. This figure shows the curves of the ideal gain (G_1), the implemented gain (G_{1_p}) and the measured gain.

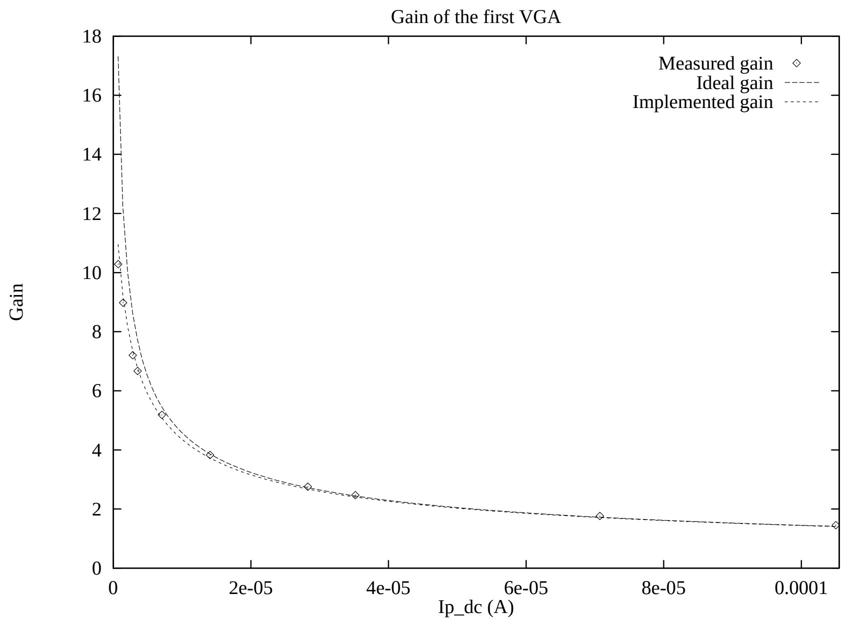

Figure 6. Gain of the first VGA versus *dc* photocurrent.

The measured values are in agreement with the expected implemented gain. The difference between the expected gain and the measured values does not exceed 10%. The difference between the measured gain and the ideal gain of VGA_1 is acceptable ($\leq 9.1\%$) for induced *dc* photocurrents larger than about 20 $\mu A/cm^2$. Regarding to the design considerations presented in section 2.2, it is shown that the implemented VGA_1 presents a measured gain near the ideal values for a large range of illumination environments.

3.2 Experimental results of the second VGA

Figure 7 displays the gain of the second VGA versus its amplitude input voltage, V_{S_2}, which is proportional to the SNR. This figure shows the curves of the ideal gain (G_2), the implemented gain (G_{2_p}) and the measured gain of VGA_2.

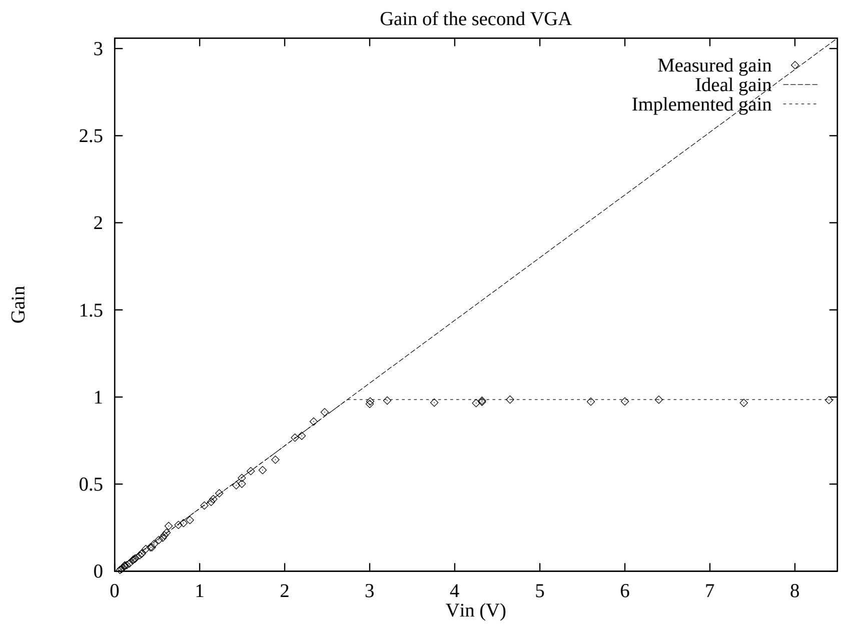

Figure 7. Gain of the second VGA versus its input voltage.

The obtained results show that the measured values are in agreement with the expected gain G_{2_p}. The difference between the expected gain and the measured gain values does not exceed 18%. For V_{S_2} larger than 2.75 V the projected and measured gain values of VGA_2 are in disagreement with the ideal gain described by equation 9. However, as it was explained in section 2.2, for large values of the SNR the gain of the second VGA does not need to fit the ideal gain.

3.3 Experimental Results of the Global VGA

Figure 8 presents the gain of the global VGA versus $\langle i_S \rangle / \sigma^2$. It presents the curves of the ideal gain (equation 3), the implemented gain (equation 19) and the measured gain values of the global VGA.

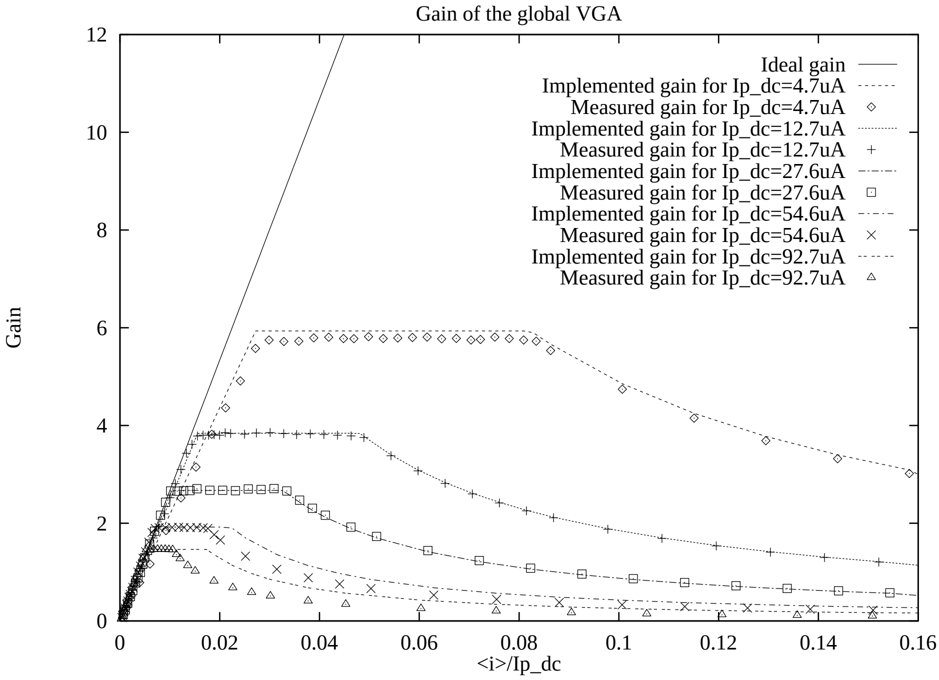

Figure 8. Gain of the global VGA versus $\langle i_S \rangle / \sigma^2$.

These measurements were executed under different conditions of SNR considering five typical *dc* photocurrents. As an outcome of the previous results, the measured values for the global gain must be in agreement with the ideal gain for $I_{p_{dc}} > 20\,\mu A/cm^2$ and SNR < 60. Indeed, for $I_{p_{dc}} = 13.4\,\mu A/cm^2$ and SNR < 60, the measured values are distant from the ideal values from about 22.2% to about 27.2%. For the other cases considered $\left(I_{p_{dc}} \geq 36\,\mu A/cm^2\right)$ the difference between the ideal gain and the measured gain values does not exceed 10%.

4. FURTHER STUDIES

During this work it was assumed that in a typical room the shot-noise is the main source of noise and that it is always higher than the receiver thermal noise. However, under some ambient light conditions, the thermal noise can be higher than the shot-noise. Thus, the contribution of the receiver thermal noise must be included during the gain definition of the variable gain amplifier. Also, the definition of the required dynamic range of the second VGA, presented in section 2.2, may be excessive. Indeed, assuming that the optical interference is solved through the utilisation of appropriate signal processing, the dynamic range of the second VGA may be, largely, reduced.

5. CONCLUSIONS

We have presented the design and implementation of a maximal-ratio angle-diversity receiver for optical wireless communication systems. The overall gain of the VGA was implemented by a cascade of two VGAs minimising dynamic range requirements through an innovative topology. The first one provides a gain inversely proportional to the *rms* shot noise and the second one a gain proportional to the SNR referred to the input of the front-end. The global VGA produces the required gain which is proportional to the average desired signal and inversely proportional to the shot noise mean square value. Measurements on the implemented prototype show very good agreement with the projected gain and are close to the ideal gain of a maximal-ratio receiver making the proposed techniques suitable for maximal-ratio angle-diversity receivers.

ACKNOWLEDGEMENTS

The first author would like to JNICT (Junta Nacional de Investigação Científica e Tecnológica) for its financial support through a Ph.D. grant BD/2599/93. Thanks are also due to Fundação Luso-Americana para o Desenvolvimento and Fundação Calouste Gulbenkian.

REFERENCES

1. F. R. Gfeller, U. H. Bapst, “Wireless In-House Data Communications Via Diffuse Infrared Radiation”, Proceedings of the IEEE, Vol. 67, No. 11, pp. 1474-1486, Nov. 1979.
2. C. J. Georgopoulos, S. H. Soultanidis, “Design of Manchester-PCM/demodulation circuitry for in-house wireless infrared communication system”, International Journal of Optoelectronics, Vol. 8, No. 1, pp. 39-48, 1993.
3. A. R. Tavares, A. C. Moreira, C. R. Lomba, L. V. Moreira, R. T. Valadas, A. O. Duarte, “Experimental Results of a 1Mbps IR Transceiver for Indoor Wireless Local Area Networks”, *COMCON V - International Conference on Advances in Communication & Control*, pp. 717-727, Crete, Greece, Jun. 26-30, 1995.
4. F. R. Gfeller, P. Bernasconi, W. Hirt, C. Elisii, B. Weiss, “Dynamic Cell Planning for Wireless Infrared In-House Data Transmission”, In *International Zurich Seminar on Digital Communications*, pp. 261-272, Springer-Verlag, Zurich, Switzerland, Mar. 8-11, 1994.
5. R. T. Valadas, A. M. Duarte, “Sectored Receivers for Indoor Wireless Optical Communication Systems”, In PIMRC’94 - *The Fifth IEEE International Symposium on Personal, Indoor and Mobile Radio Communications*, pp.1090-1095, The Hague, Netherlands, Sep. 18-23, 1994.
6. A. P. Tang, J. M. Kahn, Keang-Po Ho, “Wireless Infrared Communication Links Using Multi-Beam Transmitters and Imaging Receivers”, ICC’96 - *IEEE International Conference on Communications*, Dallas, Texas, Jun. 23-27, 1996.
7. A. R. Tavares, R. T. Valadas, A. O. Duarte, “Performance of an Optical Sectored Receiver for Indoor Wireless Communication Systems in Presence of Artificial and Natural Noise Sources”, in *Wireless Data Transmission*, Proc. SPIE 2601, pp. 264-273, Philadelphia, Pennsylvania, Oct. 23-25, 1995
8. C. T. Lomba, R. T. Valadas, A. O. Duarte, “Sectored Receivers to Combat the Multipath Dispersion of the Indoor Optical Channel”, In PIMRC’95 - *The Sixth IEEE International Symposium on Personal, Indoor and Mobile Radio Communications*, Vol. 1, pp. 321-325, Toronto, Canada, Sep. 27-29, 1995.
9. A. C. Moreira, R. T. Valadas, A. O. Duarte, “Characterisation and Modelling of Artificial Light Interference in Optical Wireless Communication Systems”, In PIMRC’95 - *The Sixth IEEE International Symposium on Personal, Indoor and Mobile Radio Communications*, Vol. 1, pp. 326-331, Toronto, Canada, Sep. 27-29, 1995.
10. A. C. Moreira, A. R. Tavares, R. T. Valadas, A. O. Duarte, “Modulation Methods for Wireless Infrared Transmission Systems - Performance under Ambient Light Noise and Interference”, in *Wireless Data Transmission*, Proc. SPIE 2601, pp. 226-237, Philadelphia, Pennsylvania, Oct. 23-25, 1995
11. A. C. Moreira, R. T. Valadas, A. O. Duarte, “Reducing the Effects of Artificial Light Interference in Wireless Infrared Transmission Systems”, in *IEE Colloquium - Optical Free Space Communication Links*, pp. 5/1-5/9, London, UK, Feb. 19, 1996